Study of the cutting properties of a composite material based on Al_2O_3 with 15 wt% SiC nanopowders

A.G. Mamalis,[1] V.P. Nerubatskyi,[2,*] E.S. Gevorkyan,[2,3] M.V. Kislitsa[4] and D.A. Hordiienko[2]

[1] *National Centre for Scientific Research "Demokritos", Athens, Greece*
[2] *Ukrainian State University of Railway Transport, Kharkiv, Ukraine*
[3] *Kazimierz Pulaski University of Technology and Humanities, Radom, Poland*
[4] *V. N. Karazin Kharkiv National University, Ukraine*

Cutting inserts obtained by electrosintering aluminum oxide and silicon carbide nanopowders have good mechanical properties and high thermal conductivity. Comparative tests of plates made of a composite of Al_2O_3 with 15 wt% SiC (As15-6) were made. The material enables finishing and semi-finishing speeds to be doubled in comparison with plates made of oxide and oxide–carbide cutting ceramics. It has been established that the formation of microcracks at grain boundaries as a result of pore formation and creep in the surface layers leads to chipping of the cutting edge. The high chipping resistance of these As15-6 ceramics is due to their high dispersion and the presence of inordinate mechanical stresses around the SiC grains.

Keywords: aluminum oxide, nanopowder, silicon carbide, sintering, wear resistance

1. Introduction

The development of new composite materials for instrumental purposes is an important step in the development of machine-building and other material-intensive industries [1]. Currently, there is a wide range of difficult-to-machine alloys, and the correct selection of the tool material for their processing is of great importance, as it increases the quality of the surface treatment of the product, making it possible to eliminate some stages of post-turning processing, and reduces tool wear. It should be noted that many technologies for obtaining materials are quite expensive, and simplifying the process of obtaining them is also relevant [2].

* Corresponding author. E-mail: NVP9@i.ua

Nanotechnology Perceptions **19** (2023) 68–79
Received 8 March 2023; *accepted* 30 March 2023

doi: 10.4024/N01MA23A.ntp.19.01

Many years of experience show that ceramic materials are extremely promising [3, 4]. Ensuring the necessary complex of attributes (such as strength, wear resistance and thermal conductivity) requires the development of sound technological bases for obtaining new ceramic materials.

Prediction of properties is the main problem in the creation of new materials and is related to the fundamental "structure–properties" problem, the solution of which involves solving a number of subordinate problems related to chemical composition and manufacturing technology.

An increase in wear resistance, which is very important for ceramic materials, is possible if composite polycrystalline materials with a fine structure are obtained. The use of nanosized powder materials is promising in this regard [5, 6]. Since nanomaterials can significantly differ in their properties and behaviour from coarsely dispersed particles of the same material, it is necessary to conduct research to demonstrate the peculiarities of the use of such materials in the manufacture of ceramic composites and form the basis for developing a system for predicting the properties of nanocomposites. The high activity of nanosized powders, which is due to the extensive surface and excess surface energy, requires the use of intensified manufacturing modes [7, 8]. It is possible to increase the speed of consolidation due to the use of new methods; for example, electroconsolidation—sintering in an electric field [9, 10]. This should reduce the duration of consolidation, increase homogeneity and, as a result, yield a high-density composite with a fine-grained structure.

The development of material for the manufacture of cutting plates for mechanized processing requires, in addition to good mechanical properties (strength and crack resistance), the study of thermophysical properties (thermal conductivity), due to the complex temperature conditions experienced by the tool. A material capable of working in difficult conditions (high temperature, exposure to high forces, subjected to friction) can be used in other fields as well—for the manufacture of parts of gas turbine engines, thermal abrasive nozzles and various sealing elements—which significantly increases the expediency of its development [11, 12].

The most important attribute of tool materials is their wear resistance [13]. It depends on wear processes that occur under certain cutting modes with certain workpieces. At the moment of metal cutting, the stress and temperature at the front corner of the cutter reach such values that jamming occurs in a plastic state between the tool and the reverse side of the chip (i.e., the workpiece), and the movement of the chip relative to the tool creates a zone of intensive cutting in the chip, not far from the surface of its separation from the tool. This generates heat, which partially goes into the chip, but can raise the temperature of some parts of the tool up to 1000 °C [14].

Due to the high temperatures, tool wear processes can be not only mechanical but also chemical [15, 16]. Abrasive wear occurs during the mechanical impact of hard particles [17], hence the material of the tool must be hard and at the same time possess sufficient fracture toughness. When the wear chamfer on the rear surface reaches a certain size, staining and chipping of the cutting edge occurs. The intensity of such marking and chipping of the cutting edge is determined by the dynamic properties of the machine, the processing modes and the structure of the cutting material [18, 19].

2. Experimental conditions

α-Al_2O_3 micropowders from LLC "Khimlaborreaktiv" (Kyiv, Ukraine) and Al100 nanopowders produced by spray drying by NANOE (France) with a purity of 99.9% were used. Tables 1 and 2 show the main physical properties of the powders, as well as data on their chemical compositions.

Table 1. Main properties of the Al100 powder.

Parameter	Value
Loss on ignition (wt%)	3/1
Average crystallite size/nm	150
Free density/g cm^{-3}	1.1
Minimum purity (%)	99.9
Alpha phase (%)	100
Specific surface area/m^2 g^{-1}	15 ± 2
Granule size (d50)/μm	35
Purity	Al100
Al_2O_3 + MgO (wt%)	< 99.9
MgO (ppm)	1000
Na_2O (ppm)	< 80
SiO_2 (ppm)	< 40
Fe_2O_3 (ppm)	< 20
K_2O; CaO (ppm)	< 10

Table 2. Main properties of SiC nanopowder brand # 4629HW manufactured by Nanostructured & Amorphous Materials (USA) (CAS # 409–21–2).

Parameter	Value
Colour	grey-green
Crystalline form	cubic (3C)
Particle size/nm	80…100
Specific surface area/m^2 g^{-1}	20…30
SiC content (%)	99
Si (%)	69.1
Free Si (%)	0.051
Free C (%)	0.35
Al (%)	0.003
Mg (%)	0.002
Fe (%)	0.012
C (%)	28.94
O (%)	0.53
Ca (%)	0.021

The cutting ceramic composite As 15-6 (SiC with 15 wt% Al_2O_3 was sintered at 1500 °C, pressure 40 MPa, holding time 3 min.

3. Results and discussion

Investigation of the properties of As15-6 was made in the process of turning the thermally treated steels 45 (40…45 HRC), HVG (58…60 HRC), ShH15 (58…60 HRC); and cast iron VCh45 (38…40 HRC). The results were compared with an oxide ceramic (VO-13), oxide–carbide ceramics (VOK-60, VOK-71), and an oxide–nitride ceramic (Kortinit). The comparison included the working mode within the ranges $v \times f \times a$ = 100…300 m/min × 0.085…0.3 mm/rev × 0.1…0.5 mm, where v is tool speed, f is feed and a is cutting depth. Figs 1 to 4 present the results in the form of dependencies between cutting strength and cutting speed for different cutting modes, and also dependencies between flank wear and cutting time. Cutting strength was determined as the time over which this wear reached the value h = 0.3 mm.

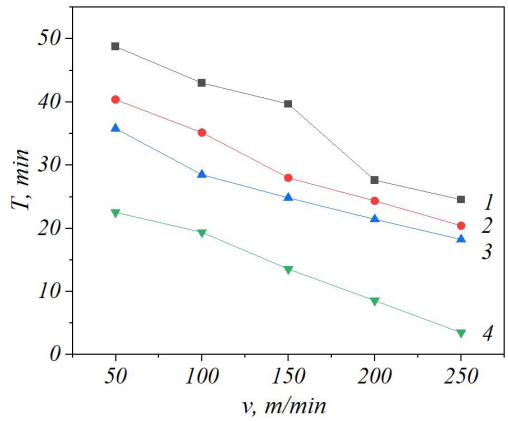

Figure 1. Dependency of wear resistance (quantified as tool life T) of ceramic cutting plates on cutting speed during treatment of steel ShH15 (58…60 HRC): *1*, As15-6; *2*, ONT-20; *3*, VOK-60; *4*, VO-13 (cutting mode $f \times a$ = 0.15 mm/rev × 0.2 mm, where f is feed and a is cutting depth).

In the process of turning rolls of hardened steels HVG and ShH15 with cutting parameters $v \times f \times a$ = 120 m/min × 0.1 mm/rev × 0.2 mm the cutting strength of composite As15-6 was about the same level as that of VOK-71 plates, amounting to about 65 min. The roughness of the surface was R_a = 0.70. When the feed reached f = 0.25 mm/rev the strength of the plates of As15-6 decreased twofold, and for the plates of VOK-71 fourfold; the plates of VOK-60 spalled within the first seconds of turning. When the cutting speed reached 200 m/min the strength of the plates of As15-6 composite was 15 min; it was five times less than the strength of the plates of VOK-71.

Fig. 2 presents the dependency between flank wear of the cutting edge on the turning time for some cutting plates of various materials; wear intensities of plates of oxides and As15-6 are compared. One of the tasks in developing new composite ceramic cutting materials is to obtain better thermal and physical properties to provide favourable temperature conditions for cutters working at higher processing speeds. The thermal conductivity of the material obtained ($\alpha = 9.4 \cdot 10^{-6}$ m^2/s) exceeded those of the existing oxide–carbide equivalents at least 1.5 times, ensuring that heat removal rate is higher in the cutting zone; this is very important for ceramics that are heat-sensitive, and the consequences are manifest in Fig. 2.

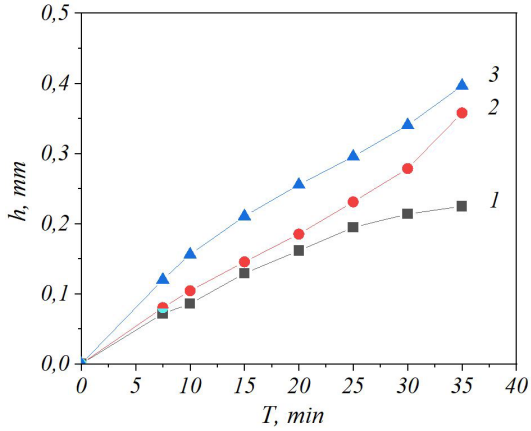

Figure 2. Dependency of flank wear *h* on the processing time for steel 45 (40…45 HRC) plates of: *1*, As15-6; *2*, VOK-71; *3*, VO-13 (cutting mode $v \times f \times a$ = 200 m/min × 0.085 mm/rev × 0.2 mm).

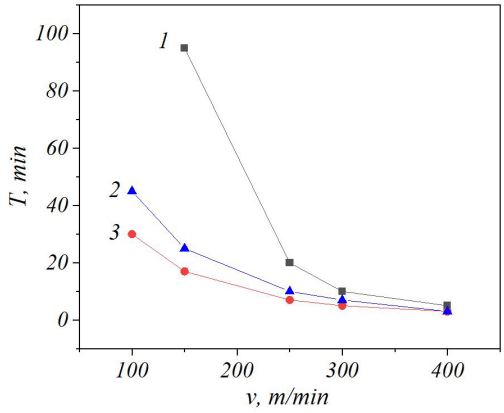

Figure 3. Dependency of the wear resistance of cutting ceramic plates on the cutting speed during processing of cast iron VCh45: *1*, As15-6; *2*, VOK-71; *3*, ONT-20 (cutting mode $f \times a$ = 0.2 mm/rev × 0.5 mm).

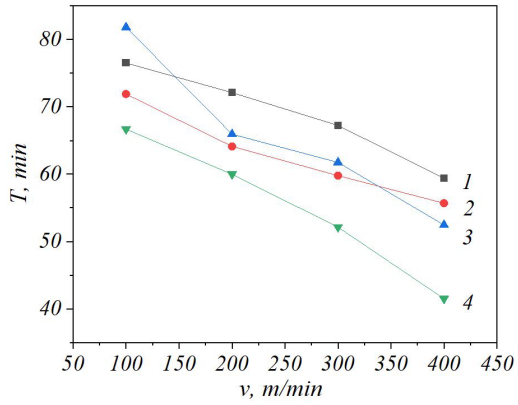

Figure 4. Dependency of ceramic cutter plate strength during turning steel 45 (40…45 HRC) on cutting speed: *1*, As15-6; *2*, ONT-20; *3*, VOK-71; *4*, VO-13 (cutting mode $f \times a$ = 0.085 mm/rev × 0.2 mm).

The wearing of cutting ceramics is accompanied by the creation of a hole on the rake face and a dimpled zone on the flank face (Fig. 5). Our results demonstrate that the wear of cutting ceramic As15-6 can be considered through universal wear dependencies of the cutting instrument [20]. After diamond turning, the grains in the oxide, nitride and carbide phases of the ceramic have a certain dislocation density; in the process of external friction during cutting the dislocation density in the grains increases.

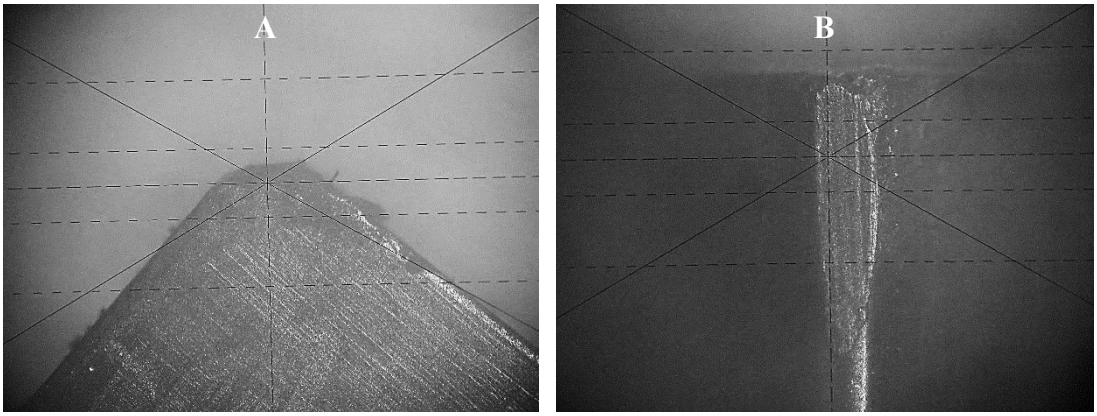

Figure 5. Wear of the rake (A) and the flank (B) faces on the cutting edge of an As15-6 plate after testing.

The analysis of microphotographs of the wear surface demonstrates that wear of the As15-6 ceramic is concomitant with microdeterioration of the grains as a result of an increase in dislocation density up to critical, cyclic slacking and grain breakaway.

Fractographic analysis shows the predominance of the grain-boundary fracture mechanism (intercrystalline), while the fracture of big grains is transcrystalline (Fig. 6). The development of microcracks on the grain boundaries due to pore formation and creep in the surface layers leads to spallation on the cutting edge. High spallation resistance of As15-6 ceramic is conditioned by its high dispersity and presence of excess mechanical stresses around the SiC grains.

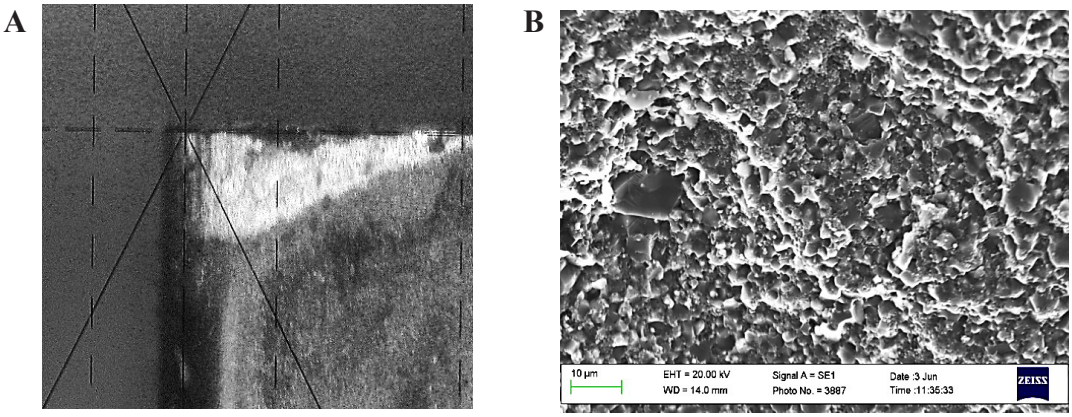

Figure 6. Cutting edge (A) and fracture pattern (B) of a cutting plate of As15-6 composite.

After the diamond turning the surface layer of the ceramic is solid up to a depth of 2…5 μm and without high internal stresses in the volume. The porosity of As15-6 ceramic does not exceed 1%; the pores are round, which also decreases stress concentration in the volume (Fig. 7).

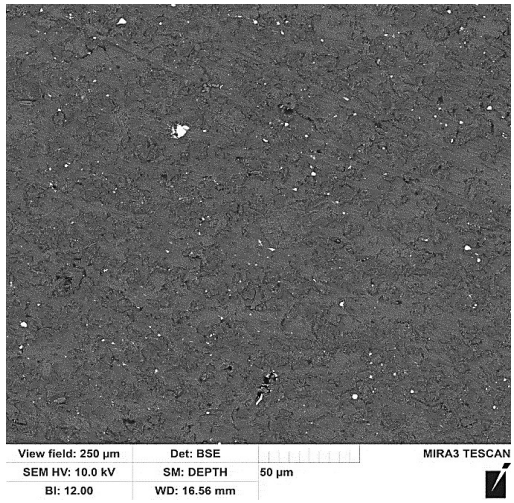

Figure 7. Surface structure of As15-6 composite after diamond turning.

Structural analysis for ceramics VO-13, VOK-60, VOK-71 and ONT-20 with scanning electron microscopy demonstrates that these instrumental materials can be considered as disperse-reinforced materials [21, 22]. According to the grade of the ceramic, its matrix is hardened with particles of oxides and carbides (TiC, TiN, ZrO_2 etc.) [23, 24]. The material is reinforced with SiC particles. The size of Al_2O_3 particles in ceramic VO-13 exceeds 3 μm.

In an oxide–carbide ceramic the size of the Al_2O_3 grains reaches 2...5 μm, and those of TiC reach 0.2…0.7 μm. The size of reinforcing particles in As15-6 is 50…100 nm. The content of reinforcing particles (TiC, TiN, SiC) in ceramics varies: for example, in the VOK-60 oxide–carbide ceramics it reaches 40 wt%, but in As15-6 it is only 15 wt%. The physical and mechanical properties of As15-6 and some cutting materials are given in Table 3.

Table 3. Physical and mechanical properties of some cutting ceramics.[a]

Name	Method of obtaining	HRA	ρ/ g cm^{-3}	σ/ GPa	K_{IC}/ MPa m$^{1/2}$	λ/ W m^{-1} K^{-1}	Grain size/ μm
CC620	Hot pressing	93	3.97	0.48	6.1	–	2
VO-13	Sintering	92	3.95	0.50	3.5	20	3…4
VOK-60	Hot pressing	94	4.30	0.60	4.2	22	2…3
ONT-20	Hot pressing	90…92	4.39	0.64	4.5	–	2
VOK-71	Hot pressing	92…93	4.52	0.65	5.6…6.0	22	2…3
As15-6	Hot pressing	94	3.83	0.85	6.5	23	1…2

[a] HRA is Rockwell hardness A scale, ρ is density, σ is bending strength, K_{IC} is the crack resistance coefficient and λ is thermal conductivity.

Disperse reinforcement of materials is determined by the morphology and the size of the particles in the reinforcing phase, the content, and the strength of interphase boundaries [25, 26]. This strength depends on the ratio of the elasticity coefficients of the reinforcing phase and the matrix, their thermal expansion coefficients, and the solubility in the reinforcing phase in the matrix. The higher the ratio of the elasticity coefficients in the matrix and reinforcing phases, the higher the stress concentration on the interphase boundaries. Table 4 gives the ratio of the elasticity coefficients of the reinforcing phases to the elasticity modulus of the matrix, and the ratio of the thermal expansion coefficients.

Table 4. Ratios of elasticity coefficients and thermal expansion coefficients.

Ratios of Young's moduli E and coefficients of thermal expansion α	TiN / Al_2O_3	TiC / Al_2O_3	SiC / Al_2O_3
E_1 / E_2	0.7	1.3	0.9
α_1 / α_2	1.2	1.0	2.0

Table 4 shows that in the aluminium oxide matrix, silicon carbide gives a higher stress concentration on the interphase boundary than titanium carbide or titanium nitride. Besides, SiC grains are more disperse; therefore they are more coherent with the matrix. Thus, the high wear resistance of As15-6 during the processing of hardened steels can be explained by the higher strength of the interphase boundaries.

A potential reaction and the type thereof between the material being processed and the structural components of the cutting ceramic can be predicted on the basis of calculation of thermodynamic potential.

The present results demonstrate that the temperature in the cutting zone in fine surface layers can reach the $Fe_\alpha \rightarrow Fe_\gamma$ phase transition temperature of iron. High pressures initiate dissociation of iron carbide. Thus, the main elements diffusing into the surface layers of the ceramics would be ionized iron and carbon, as they are in austenite. However, calculation demonstrates that for the reaction $Al_2O_3 + 2Fe \rightarrow 2Al + Fe_2O_3$ the thermodynamic potential is positive over a wide range of temperatures and the reaction is energetically unfavourable.

Reactions with carbon such as $2Al_2O_3 + 9C \rightarrow Al_4C_3 + 6CO$ can run at temperatures > 1800 °C, which is beyond the working temperature of the cutting tools. At a temperature of 1100…1300 °C, reaction between Al_2O_3 and the silicon, magnesium or calcium (their oxides) contained in steel is possible.

X-ray analysis does not reveal carbides and pure Fe and Al in the chip and materials under processing as the result of potential renovation of their oxides. However, contact area strata of the material being processed contains the oxides FeO and Fe_2O_3.

Experimental data were used to obtain the empirical mathematical dependencies of the main strength characteristics, notably the microhardness H_V and the crack resistance coefficient K_{IC}:

$$H_V\left(T,x\right) = A_0 + \frac{A}{D_T \cdot D_x}, \tag{1}$$

where

$$D_T = n + \left(\frac{T - T_C}{W_T}\right)^2 - b_T \cdot \left(\frac{|T - T_C| + T - T_C}{2 \cdot W_T}\right)^2; \tag{2}$$

$$D_x = \frac{1}{n} + \left(\frac{x - x_C}{W_x}\right)^2 - b_x \cdot \left(\frac{x - x_C - |x - x_C|}{2 \cdot W_x}\right)^2; \tag{3}$$

$$K_{\mathrm{IC}}(T,x) = A_0 + \frac{A}{\left[n + \left(\frac{T - T_C}{W_T}\right)^2\right] \cdot \left[\frac{1}{n} + \left(\frac{x - x_C}{W_x}\right)^2\right]}, \tag{4}$$

where T is here the sintering temperature, x is the SiC content in the primary mixture in wt%; A_0 is the tool–chip contact area before wear; A is the area after wear; W_T and W_x are coefficients giving the influence of T and x on the width of the tool–chip contact area, b_T, b_x are the coefficients of thermal conductivity, and n is the coefficent of heat partition. These equations (1)–(4) are three-dimensional variants of the Lorentz function [27]. Numerical values of the coefficients for these equations are given in Table 5.

Table 5. Coefficients for equations (1)–(4).

Factor	A_0	A	T_C/ °C	W_T	x_c (%)	W_x	b_T	b_x	n
for H_V	8.0	16.8	1620	180	15.1	30.0	0.8	0.5	1.3
for K_{IC}	3.5	3.3	1560	120	15.0	0.6	–	–	1

Plots of these functions are given in Fig. 8. They show that the optimal amount of SiC additive in the composite under consideration is 15 wt%, and the optimal consolidation temperature for this composition is 1600 °C. The inclination of planes can be used for estimation of the impact of each primary parameter on the hardness H_V and stress intensity coefficient K_{IC}.

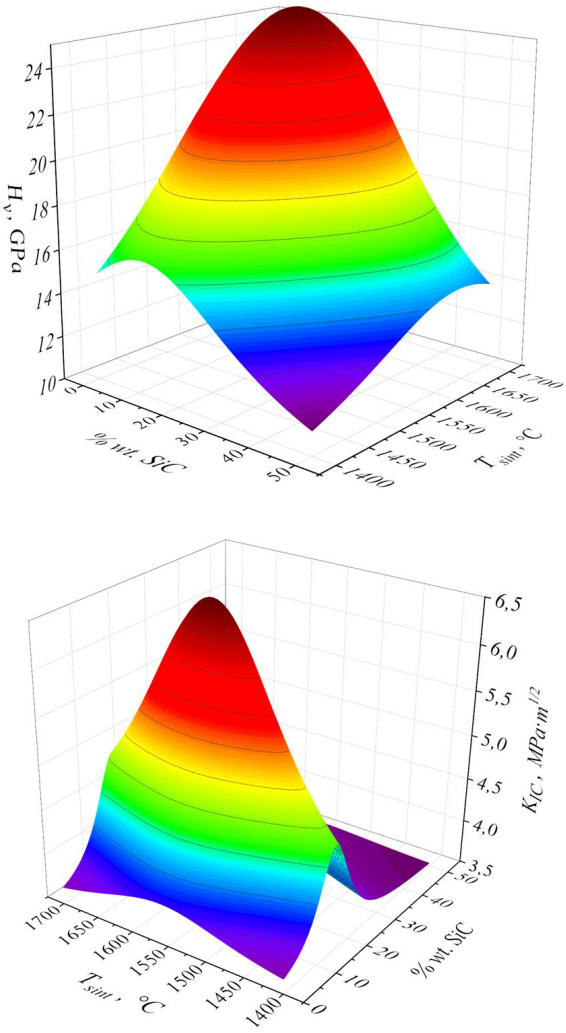

Figure 8. Dependency of the microhardness H_V (upper) and the stress intensity coefficient K_{IC} (lower) on the sintering temperature T_{sint} and SiC content in the Al_2O_3–SiC system.

4. Conclusions

Comparative studies of various cutting ceramic materials show that the main reasons for the high wear resistance of oxide–carbide ceramics when processing steels are their fine-grained structure and the substructural and dispersed strengthening mechanism. In white Al_2O_3 ceramics, the grains contain dislocations; hence the grains are not capable of storing deformation energy, as a result of which microdestruction of the Al_2O_3 grains occurs in the surface layers of the tool. It follows that increasing the resistance to brittle fracture of oxide–carbide ceramics and the stability of their cutting properties can be achieved by reducing the size of the grains in the matrix, which is realized when using carbide (TiC, SiC) additives.

Tests of the composite material, made in this work, during turning of high-strength alloys demonstrate that it allows the speed of finishing and semifinishing to be increased twofold compared to plates made of oxide and oxide–carbide cutting ceramics. The novel nanocomposite material is four times higher than domestic high-speed steel and two times higher than modern cutting materials based on Al_2O_3 of foreign production, in terms of thermomechanical properties. Further improvement of performance and reliability of As15-6 ceramics can doubtless be achieved by optimization of the diamond processing régime, polishing (smoothing of irregularities), spraying of the defective surface layer, as well as by mechanically dampening the tool in the normal direction. The latter can be achieved by increasing the thickness of the plates.

References

1. E.S. Gevorkyan, M. Rucki, A.A. Kagramanyan and V.P. Nerubatskiy, Composite material for instrumental applications based on micro powder Al_2O_3 with additives nano-powder SiC. *International Journal of Refractory Metals and Hard Materials* **82** (2019) 336–339.
2. B. Zeiler, A. Bartl and W.-D. Schubert, Recycling of tungsten: Current share, economic limitations, technologies and future potential. *International Journal of Refractory Metals and Hard Materials* **98** (2021) 105546.
3. O. Guillon, Ceramic materials for energy conversion and storage: A perspective. *International Journal of Ceramic Engineering and Science* **3** (2023) 100–104.
4. E.A. Levashov, V.V. Kurbatkina, E.I. Patsera, Y.S. Pogozhev, S.I. Rupasov and A.S. Rogachev, Self-propagating high-temperature synthesis of promising ceramic materials for deposition technologies of functional nanostructured coatings. *Russian Journal of Non-Ferrous Metals* **51** (2010) 403–433.
5. E. Gevorkyan, V. Nerubatskyi, Yu. Gutsalenko, O. Melnik and L. Voloshyna, Examination of patterns in obtaining porous structures from submicron aluminum oxide powder and its mixtures. *Eastern European Journal of Enterprise Technologies* **6** (2020) 41–49.
6. E. Gevorkyan, A. Mamalis, R. Vovk, Z. Semiatkowski, D. Morozow, V. Nerubatskyi and O. Morozova, Special features of manufacturing cutting inserts from nanocomposite material Al_2O_3-SiC. *Journal of Instrumentation* **16** (2021) P10015.
7. A. Aimable, N. Jongen, A. Testino, M. Donnet, J. Lemaître, H. Hofmann and P. Bowen, Precipitation of nanosized and nanostructured powders: process intensification and scale-out using a segmented flow tubular reactor (SFTR). *Chemical Engineering and Technology* **34** (2010) 344–352.
8. G. Vega, A. Quintanilla, N. Menendez, M. Belmonte and J.A. Casas, 3D honeycomb monoliths with interconnected channels for the sustainable production of dihydroxybenzenes: towards the intensification of selective oxidation processes. *Chemical Engineering and Processing—Process Intensification* **165** (2021) 108437.
9. Z. Krzysiak, E. Gevorkyan, V. Nerubatskyi, M. Rucki, V. Chyshkala, J. Caban and T. Mazur, Peculiarities of the phase formation during electroconsolidation of Al_2O_3–SiO_2–ZrO_2 powders mixtures. *Materials* **15** (2022) 6073.
10. E.S. Gevorkyan, V.P. Nerubatskyi, R.V. Vovk, V.O. Chyshkala and M.V. Kislitsa, Structure formation in silicon carbide–alumina composites during electroconsolidation. *Journal of Superhard Materials* **44** (2022) 339–349.
11. V.A. Lebedev, O.M. Dubovyy, S.A. Loi and S.V. Novykov, Features of studying coating strength and methods increasing its indicators with plasma spraying working bodies of gas turbine engines and plants. *Metallophysics and Advanced Technologies* **44** (2022) 1293–1311.

12. V. Sychuk, O. Zabolotnyi and A. McMillan, Developing new design and investigating porous nozzles for abrasive jet machine. *Powder Metallurgy and Metal Ceramics* **53** (2015) 600–605.
13. G.M. Sorokin and V.N. Malyshev, Criterion of wear resistance for ranking steels and alloys on mechanical properties. *International Journal of Material and Mechanical Engineering* **1** (2012) 114–120.
14. Rezhushchie instrumenty, osnashchennye sverkhtverdymi i keramicheskimi materialami, i ikh primenenie: Spravochnik / V.P. Zhed', G.V. Borovskii, A.Ya. Muzykant, G.M. Ippolitov. Moscow: Mashinostroenie (1987) (in Russian).
15. J. Qiu, S. Zhang, B. Li, Y. Li and L. Wang, Research on tool wear and surface integrity of CFRPs with mild milling parameters. *Coatings* **13** (2023) 207.
16. L. Zheng, W. Chen and D. Huo, Investigation on the tool wear suppression mechanism in non-resonant vibration-assisted micro milling. *Micromachines* **11** (2020) 380.
17. I. Sevim, Effect of abrasive particle size on abrasive wear resistance in automotive steels. In: *Tribology in Engineering* (ed. H. Pihtili), pp. 29–46. Intech (2013).
18. A.L. Vil'son, Vybor instrumenta i rezhima rezaniya, obespechivayushchikh minimal'nye vibratsii pri obrabotke. *Stanki i Instrument* **4** (1987) 28–30 (in Russian).
19. W. Zebala, G. Struzikiewicz and K. Rumian, Cutting forces and tool wear investigation during turning of sintered nickel-cobalt alloy with CBN tools. *Materials* **14** (2021) 1623.
20. Tablitsy fizicheskikh velichin: Spravochnik / Pod. red. akad. I. K. Kikoina. Moskva: Atomizdat (1976) (in Russian).
21. E. Gevorkyan, M. Rucki, Z. Krzysiak, V. Chishkala, W. Zurowski, W. Kucharczyk, V. Barsamyan, V. Nerubatskyi, T. Mazur, D. Morozow, Z. Siemi¹tkowski and J. Caban, Analysis of the electroconsolidation process of fine-dispersed structures out of hot pressed Al_2O_3–WC nanopowders. *Materials* **14** (2021) 6503.
22. Svoistva konstruktsionnykh materialov na osnove ugleroda: Spravochnik / Pod red. V. P. Sosedova. Moskva: Metallurgiya (1975) (in Russian).
23. E. Gevorkyan, M. Rucki, T. Salacinski, Z. Siemiatkowski, V. Nerubatskyi, W. Kucharczyk, Ja. Chrzanowski, Yu. Gutsalenko and M. Nejman, Feasibility of cobalt-free nanostructured WC cutting inserts for machining of a TiC/Fe composite. *Materials* **14** (2021) 3432.
24. E.S. Gevorkyan, V.P. Nerubatskyi, R.V. Vovk, V.O. Chyshkala, S.V. Lytovchenko, O.M. Morozova and J.N. Latosinska, Features of synthesis of $Y_2Ti_2O_7$ ceramics for the purpose of obtaining dispersion-strengthened steels. *Acta Physica Polonica A* **142** (2022) 529–538.
25. I. Razumovskii, B. Bokstein and M. Razumovsky, Approaches to the development of advanced alloys based on refractory metals. *Encyclopedia* **3** (2023) 311–326.
26. P. Ranachowski, Z. Ranachowski, S. Kudela, A. Pawe³ek and A. Piatkowski, Study of factors determinant of siliceous electrical porcelain resistance to structural degradation. *Archives of Metallurgy and Materials* **61** (2016) 1143–1150.
27. W.H. Press, S.A. Teukolsky, W.T. Vetterling and B.P. Flannery, *Numerical Recipes—The Art of Scientific Computing* (3rd edn). Cambridge: University Press (2007).